Optimizing A Communication System By Neural Circuits: The Magic Number 4 And Golden Ratio

Bo Deng[1]

Abstract: For a new class of circuit models of neurons we demonstrate here that an artificial but robust and efficient communication system can be constructed using one neural circuit as an encoder/transmitter and another as a receiver/decoder, for which metastable-plastic spike-bursts with the minimal bursting periods are used for its alphabet. We also demonstrate that the spike-bursting alphabet is frequency-modulated onto the encoder's ion pump current as the signal. We further demonstrate that for this spike-excitation-encoding-decoding (SEED) system, the quadrary alphabet tends to give the maximal transmission rate for all possible sources. We also demonstrate that by a trivial source-to-channel encoding, a binary source with the Golden Ratio distribution can be transmitted at the channel capacity of a binary SEED system.

1. Introduction. In animal nervous systems a typical neuron is connected to not just one but many other neurons. The connection from a pre-synaptic neuron to a post-synaptic neuron is more or less understood in structure but more than complicated in its effect. Once the pre-synaptic neuron is excited, an action potential is fired to trigger its synapses to release neural transmitters to the dendrites of its post-synaptic neurons. The neural transmitters can be either inhibitory or excitatory and their electro input in either current or potential to their post-synaptic neurons is only added to the total from all other pre-synaptic neurons. The response of a post-synaptic neuron is graded — only when it crosses a threshold does it fire an action potential along its axon, so on and so forth. Further complicating the picture, the axonal action potential appears to have a fixed profile but the membrane potential across the soma can exhibit spike-bursts with varying number of spikes. That is, the effect of one neuron to another neuron cannot be understood in the absence of other pre-synaptic neurons, the effect of a pre-synaptic neuron to the spike-bursts of its post-synaptic neurons in particular. Nevertheless, one can think a neuron's graded response in spike-bursts, which are thought to represent information, to be the effect of all pre-synaptic neurons. It is with this understanding that the communication system we will introduce below is artificial.

This paper is about how to best construct a communication system using one neuron circuit model as an encoder/transmitter and another neuron circuit model as a receiver/decoder. In this setting the transmission line of the system cannot be interpreted as a single axon but rather some aggregated effect of all pre-synaptic axons, and the transmitter not as one neuron but some aggregated effect of all pre-synaptic neurons. As a result we seek to understand only the information rate and information capacity when bursting spikes are used for an encoding alphabet on the cell body.

[1]Department of Mathematics, University of Nebraska-Lincoln, Lincoln, NE 68588. Email: bdeng1@math.unl.edu

In Claude E. Shannon's mathematical model for communication ([12]), there is an information source which produces messages in sequences of a source alphabet, an encoder/transmitter which translates a message into a signal in time-series of a channel alphabet, a channel through which the signal is transmitted to a receiver/decoder, which usually performs an inverse operation to extract the message from the signal. The transformation from the source alphabet to the channel alphabet is referred to as a source-to-channel encoding. Any communication system is characterized by two intrinsic performance parameters. One, its mean transmission rate (in bit per time) for all possible information sources, such as your Internet connection speed for all kinds of sources, both wanted and unwanted. Two, its channel capacity which a particular information source or a particular source-to-channel encoding scheme can take advantage to transmit at the fastest source data rate.

For the neuron-to-neuron communication system considered here, we will use a new type of neuron circuit models from [5] for the system's transmitter and receiver. We will use the circuit's excitable states in spike-bursts for the system's encoding/decoding channel alphabet, and use the transmitter's active ion pump current for the system's signal waveform. The resultant system is referred to as a *SEED* system for *spike-excitation-encoding-decoding*. The objective of this paper is to construct the best SEED system satisfying the following criteria

(a) The time it takes to transmit each alphabetical k-spike burst is minimal with respect to all choices of the same k-spike class of bursts.

(b) The transmission rate is maximal with respect to all possible choices of alphabetical bases with the minimal transmitting times stipulated by (a).

The result of this paper is four-fold. First, we will show that simple, reliable, and operational SEED systems can be constructed. Second, we will show that it is because of the minimal transmitting times for the encoding spike-bursts that using the first 3 or 4 alphabetical bases in k-spike bursts maximizes SEED's transmission rate. Thirdly, we will derive the channel capacity for all SEED systems, and show in particular that for the binary SEED subsystem with an equal spike transmitting time for both bursting bases, the channel capacity is reached when the encoded source is distributed according to the Golden Ratio distribution: $p_1 + p_2 = 1$ with $p_2/p_1 = p_1/1 = \Phi = \frac{\sqrt{5}-1}{2} = 0.6180$. Fourthly, we will argue that the quadrary system and the Golden Ratio distribution are more biologically probable when the minimal base transmitting time requirement is relaxed to allow stochastic variations. Since the mathematical model of a system is less about how does the system work, but more about why is the way it does, we will speculate at the end of the paper if such preferences by the SEED systems to the quadrary alphabet and to the Golden Ratio information source are reflected by the larger nervous systems.

The paper was partially motivated by the following observation from neurophysiology. It has been well-known ([8, 13]) that neurons are capable of generating both spikes and spike-bursts but axons are only known to generate spikes (or pulses) not spike-bursts. The intriguing question is if spike-bursts do code information by neurons, then how is it transmitted by axons without each axon's exhibiting spike-bursts? The SEED model may suggest a solution to this problem: it is the

post-synaptic ion pump current that is the aggregated effect of all firing pre-synaptic neurons to encode the spike-bursts by frequency modulation. We note that this prediction, true or false, cannot be made from Hodgkin-Huxley based neuron models because they do not separate cell membrane's passive ion currents from their active ion pump currents ([5, 6]).

2. Circuit Models of Neurons and The Shortest Spike-Burst Times. We view a neuron as an information processing unit either as a signal transmitter or a signal receiver or both. A communication system must have an alphabet to code information source and each base (or letter) of the alphabet must be represented by a physical state of the system. Since a communication system is also a dynamical process in which information is coded and decoded in real time, an efficient system should process the physical alphabet states in transient, not to wait for the system to settle down to its asymptotic states. A reliable communication system, on the other hand, should have the transient alphabetical states to behave like steady states, having robust and distinct profiles for high error tolerance. In addition, a functional communication system must be able to shift from one alphabetical state to another for information encoding. A transient state behaving like a steady state is referred to as *metastable*, and the capability to internally shift from one metastable alphabet state to another is referred to as *plastic*, see [6].

A class of circuit models for neurons are found to possess this dual metastable-plastic property. The key facilitator of the property is shown to be the two-way Na^+-K^+ ion pump across neuron's cell membrane, see [6]. We will use one model type here for a prototypical illustration while all other types from [5, 6] work just as well. The circuit equations of the type are given as follows:

$$\begin{cases} CV_{\rm C}{}' = -[I_{\rm Na} + f_{\rm K}(V_{\rm C} - \bar{E}_{\rm K}) + I_{\rm Na\ pump} - I_{\rm K\ pump} - I_{\rm ext}] \\ I_{\rm Na\ pump}{}' = \lambda_{\rm Na} I_{\rm Na\ pump}[V_{\rm C} - \gamma_{\rm Na}(I_{\rm Na\ pump} - \delta I_{\rm K\ pump})] \\ I_{\rm K\ pump}{}' = \lambda_{\rm K} I_{\rm K\ pump}[-V_{\rm C} + \gamma_{\rm K}(\delta I_{\rm Na\ pump} - I_{\rm K\ pump})] \\ \epsilon I_{\rm Na}{}' = V_{\rm C} - \bar{E}_{\rm Na} - h_{\rm Na}(I_{\rm Na}). \end{cases} \tag{1}$$

The definitions of the variables and parameters are given in Table 1. The parameter δ takes only two values: 0 and 1, for which the model is referred to as the $\text{pK}^+_-\text{sNa}^+_+$ model when $\delta = 1, \gamma_{\rm Na} = \gamma_{\rm K} = \gamma$, and, respectively, as the $\text{pK}^+_{-d}\text{sNa}^+_{+d}$ model for $\delta = 0$. For the former, the Na^+ and K^+ ion pumps are coupled as one unit and for the latter, the pumps are decoupled, each operating independently from the other.

As for the IV-characteristic $I = f_{\rm K}(V)$, here are the minimal conditions: v_1, v_2 are the only critical point; ${f_{\rm K}}' < 0$ in $[v_1, v_2]$ with $\min\{{f_{\rm K}}'\} = d_{\rm K} + g_{\rm K} < 0$; and ${f_{\rm K}}' > 0$ outside $[v_1, v_2]$ with $\max\{{f_{\rm K}}'\} = g_{\rm K} > 0$; and last $f_{\rm K}(0) = 0$. Similarly, for the IV-characteristic $V = h_{\rm Na}(I)$, these are the minimal conditions: i_1, i_2 are the only critical point; ${h_{\rm Na}}' < 0$ in $[i_1, i_2]$ with $\min\{{h_{\rm Na}}'\} = 1/d_{\rm Na} + 1/g_{\rm Na} < 0$; and ${h_{\rm Na}}' > 0$ outside $[i_1, i_2]$ with $\max\{{h_{\rm Na}}'\} = 1/g_{\rm Na} > 0$; and $h_{\rm Na}(0) = 0$. There are many functions that satisfy these conditions. But, there is only a unique piecewise linear and continuous (PWLC) function satisfying these conditions for each characteristic which we will use. There are two more types of smooth curves we will refer to, one type has the sum of a linear function and an arctangent function, and the other has the form of polynomials of degree three.

Table 1: Circuit Variable and Parameter Legend

		Variables
$V_{\rm C}$	—	Membrane voltage with the default current direction being outward.
$I_{\rm Na\ pump}$	—	Outward current through the Na^+ ion pump with $I_{\rm Na\ pump} > 0$.
$-I_{\rm K\ pump}$	—	Inward current through the K^+ ion pump with $I_{\rm K\ pump} > 0$.
$I_{\rm Na}$	—	Current through Na^+'s serial passive channels.
$I_{\rm pump} = I_{\rm Na\ pump} - I_{\rm K\ pump}$	—	Net current through the parallel Na^+-K^+ ion pump.
$I_{\rm S} = I_{\rm Na\ pump} + I_{\rm K\ pump}$	—	Absolute current through the parallel Na^+-K^+ ion pump, $I_{\rm S} > 0$.
$I_{\rm ext}(t)$	—	Inward external current.
		Parameters
$\bar{E}_{\rm Na} > 0$	—	The resting potential of Na^+'s passive channels.
$\bar{E}_{\rm K} < 0$	—	The resting potential of K^+'s passive channels.
$\lambda_{_{\rm J}}$	—	Ion J's pump coefficient.
$\gamma_{_{\rm J}}$	—	Ion J's pump resistance.
		IV-Characteristics and Parameters
$I = f_{\rm K}(V)$	—	For K^+'s electro and diffusive channels in parallel, with maximal conductance $g_{_{\rm K}} > 0$, minimal diffusion $d_{_{\rm K}} + g_{_{\rm K}} < 0$, and the diffusion domination voltage range $[v_1, v_2]$. $f_{\rm K}(0) = 0$.
$V = h_{\rm Na}(I)$	—	For Na^+'s electro and diffusive channels in series, with maximal conductance $g_{_{\rm Na}} > 0$, minimal diffusion $g_{_{\rm Na}} d_{_{\rm Na}}/(d_{_{\rm Na}} + g_{_{\rm Na}}) < 0$, and the diffusion domination current range $[i_1, i_2]$. $h_{\rm Na}(0) = 0$.

Their precise forms and systematic derivations can be found in [5, 6].

Fig.1 gives a typical illustration for the phenomenon of metastability and plasticity. Fig.1(a) shows a typical spike-burst with 3 spikes per burst. It looks like an asymptotic state but in fact only a transient state. That is, if the time-series last long enough in time, the 3-spike burst will repeat itself many times but eventually change to a 2-spike burst or to a 4-spike burst, depending on the model, a typical manifestation of the metastability and plasticity. We note that as shown in [6] the voltage profile in bursting and spiking ranges remains the same for all spike-bursts, but the absolute ion pump current $I_{\rm S}(t)$ changes with the transient spike-bursts, which we now give a more detailed description below.

Let τ_k denote the burst period for a k-spike burst which both starts and ends when $V_{\rm C} = 0$ as shown in Fig.1(a). Although we instinctively want to know right away the minimum value of τ_k over the class of all k-spike bursts, it is easier to consider indirectly the average spike frequency, k/τ_k, instead. Notice that $1/\tau_k$ is the burst frequency representing the number of bursts per unit time. Since there are k spikes in the burst, the spike frequency is precisely k/τ_k, representing the number of spikes per unit time. Both are instantaneous frequencies, not including the refractory

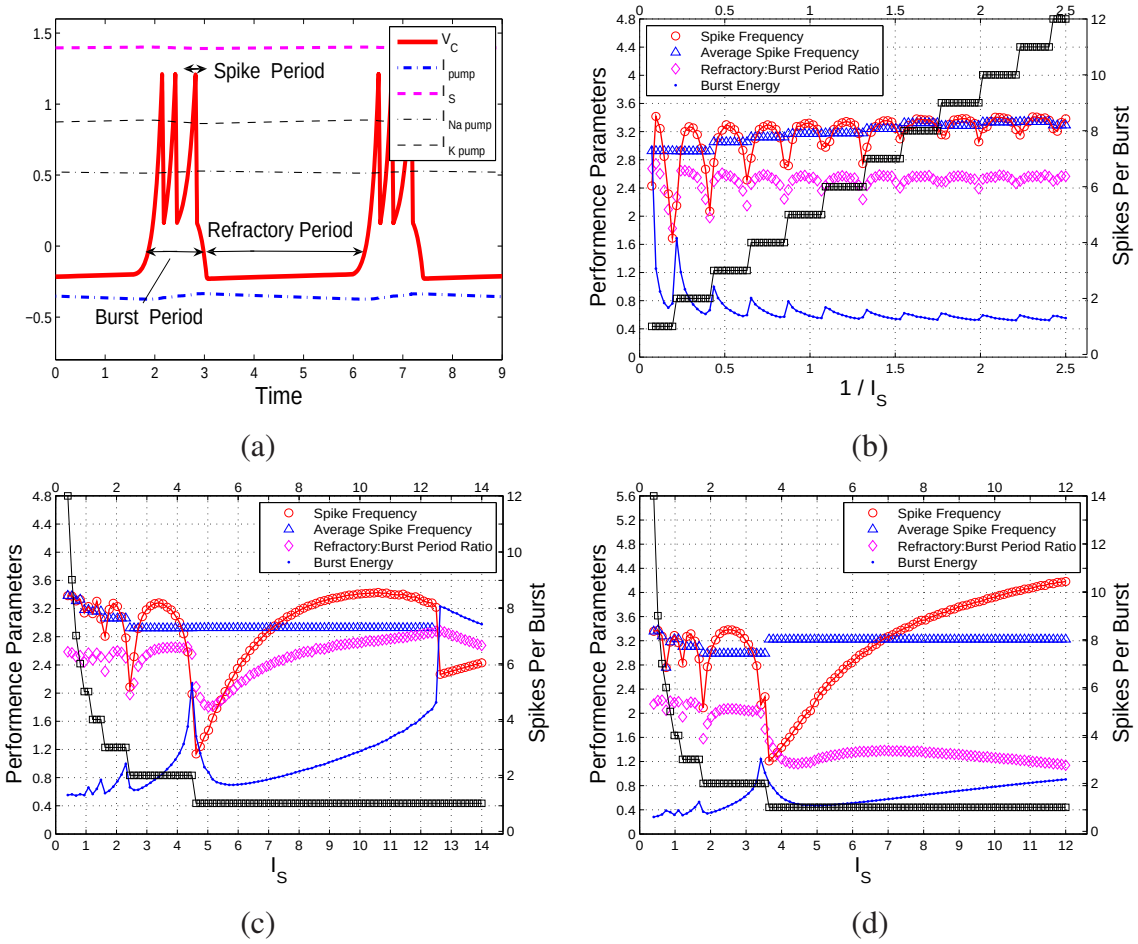

Figure 1: (a) Terminology Legend. (b) The $\text{pK}^{+}_{-}\text{sNa}^{+}_{+}$ model ($\delta = 1$ for Eq.(1)) with the PWLC IV-curves. Parameter values: $g_{\text{K}} = 1, d_{\text{K}} = -1.25, v_1 = 0.5, v_2 = 2, g_{\text{Na}} = 0.16, d_{\text{Na}} = -0.1, i_1 = .06, i_2 = 0.28, g_{\text{Cl}} = 0.01, d_{\text{Cl}} = 0, \bar{E}_{\text{Na}} = 0.6, \bar{E}_{\text{K}} = -0.7, \bar{E}_{\text{Cl}} = -0.6, \lambda_{\text{Na}} = \lambda_{\text{K}} = 0.05, \gamma_{\text{Na}} = \gamma_{\text{K}} = 0.1, \delta = 1, C = 0.01, I_{\text{ext}} = 0, \epsilon = 0.0005$. (c) The same plot as (b) except against the variable I_{S}. (d) The $\text{pK}^{+}_{-d}\text{sNa}^{+}_{+d}$ model ($\delta = 0$ for Eq.(1)) with the same PWLC IV-curves. The same parameter values as (b) except $\lambda_{\text{Na}} = \lambda_{\text{K}} = 0.1, \gamma_{\text{Na}} = 0.1, \gamma_{\text{K}} = 0.05, \delta = 0$.

period, which, to be included in the consideration later, is defined when $V_{\rm C}$ crosses 0 as shown in Fig.1(a). Thus, for a given k-spike burst class, the maximal spike frequency and the maximal burst frequency uniquely determine each other, differing only by the integer spike number k. Notice also that the maximal burst frequency and the minimal burst period uniquely determine each other, each is the reciprocal of the other. The spike-burst frequencies and periods are captured by the remaining plots of Fig.1.

Here is how Fig.1(b) is generated. For example, at a refractory point $(V_{\rm C}, I_{\rm Na\ pump}, I_{\rm K\ pump}, I_{\rm Na})(t)$ in the phase space, we only add or subtract a same amount to both ion pump currents $I_{\rm Na\ pump}, I_{\rm K\ pump}$ so that the net current $I_{\rm pump} = I_{\rm Na\ pump} - I_{\rm K\ pump}$ remains the same but the absolute amount $I_{\rm S} = I_{\rm Na\ pump} + I_{\rm K\ pump}$ is reset to any desired value. For example, if $I_{\rm S}(t_0)$ is reset so that $1/I_{\rm S}(t_0) = 1$, then the plot tells us that the subsequent burst generates 5 spikes and with its spike frequency barely lower than the maximum (at 3.3 spikes per unit time) of all 5-spike bursts. This will last awhile for some $t > t_0$ with changing spike frequency and before changing to a 4-spike or 6-spike burst. The plot only shows the frequency for the immediate, transient 5-spike burst. Similarly, if the absolute pump current is reset to a different value, say, $1/I_{\rm S}(t_0) = 0.5$, then the subsequent burst will have 3 spikes with a frequency slightly less than its own class's maximal spike frequency.

From now on, we will restrict the notation τ_k only to the *minimal* burst period for the k-spike burst class. From Fig.1(b,d) we can assume that the maximal spike frequencies are equal for all $k \geq 2$:

$$\frac{k}{\tau_k} = \frac{2}{\tau_2} := \frac{1}{\tau_*}.$$

We note that we have seen cases where the sequence $\{k/\tau_k\}$ is monotonically increasing to a limit, $1/\tau_*$, but not decreasing to $1/\tau_*$ (c.f. [6]). In other words, finding the parameters for which the condition above holds seems to be the best outcome as far as finding the maximal spike frequencies for all $k \geq 2$ spike-bursts is concerned. We also note that it is fairly easy to find the parameters to satisfy the equal maximal spike frequency condition above.

As for the maximal spike frequency, $1/\tau_1$, of the uni-spike bursts, the graphs show instead that it can be higher than the remainder absolute maximum $1/\tau_*$. Thus, for the rest of the paper we will conveniently scale τ_1 against the remainder absolute minimal spike period τ_* by a parameter α as follows:

$$\tau_1 = \alpha\tau_*, \quad \text{or} \quad \alpha = \frac{1/\tau_*}{1/\tau_1}, \quad \text{and} \quad \tau_k = k\tau_* = \frac{k}{\alpha}\tau_1 \quad \text{for} \quad k \geq 2. \tag{2}$$

Thus, for $\alpha < 1$, the uni-spike burst takes less time to transmit than the average single spike of any other burst does. It in turn corresponds to a higher $I_{\rm S}$ value than $\alpha \geq 1$ does as $\alpha = (1/\tau_*)/(1/\tau_1)$. At the special value $\alpha = 1$, the averaged spike interval is the same for all k-spike bursts with $k \geq 1$ and the minimal burst time sequence progresses exactly like the natural numbers: $\tau_1, 2\tau_1, 3\tau_1, 4\tau_1, \ldots$. For the model of Fig.1(b,c), the α value is estimated by using (2) to be approximately 0.95.

Fig.1(c) is the same plot as (b) except against the absolute pump current variable $I_{\rm S}$. Plot

(c) clearly shows that the burst frequency changes with the plastic variable $I_{\rm S}$, i.e., the burst is frequency-modulated by $I_{\rm S}$. Plot (b), on the other hand, clearly indicates that the per-burst spike number variable k is inversely proportional to $I_{\rm S}$. Fig.1(d) is the same plot as (c) except for a $\text{pK}^+_{-d}\text{sNa}^+_{+d}$ model (with $\delta = 0$ in Eq.(1)) whose α value is approximately 0.80. Notice that even though the ion pumps are structured differently, their spike-burst dynamics can be made more or less the same both qualitatively and quantitatively.

3. SEED System. From the perspective of a communication system, Fig.1's plot for the spike frequency *v.s.* the plastic variable $I_{\rm S}$ cannot be more obvious than an alphabet table: the k-spike burst of the shortest period can be uniquely accessed by an $I_{\rm S}$ value, denoted by $I_{{\rm S},\,k}$. Specifically, the following is a prototypical implementation of the SEED system using the $\text{pK}^+_-\text{sNa}^+_+$ model as an example.

Design Principles and Implementation Rules:

Alphabet: The kth alphabetical base b_k is the metastable-plastic k-spike burst of Eq.(1) with the minimal bursting time τ_k satisfying the relation (2). It starts at a refractory point P_k immediately before the burst, and ends at a refractory point Q_k shortly after the burst. The reset point P_k (from any end point Q_j) can be chosen in such a way that their $V_{\rm C}, I_{\rm pump}, I_{\rm Na}$ components remain the same for all k but different in the plastic variable $I_{{\rm S},\,k}$ for each k.

Encoder: Let $m = m_1 m_2 m_3 m_4 \cdots$ denote a message sequence with each m_i being the spike number of a spike-burst alphabetical base b_j, namely, $j = m_i$. By only resetting to $b_{m_{i+1}}$'s starting point $P_{m_{i+1}}$ at b_{m_i}'s end point Q_{m_i}, a time series $b = b_{m_1} b_{m_2} b_{m_3} b_{m_4} \cdots$ is generated by Eq.(1) to encode the message sequence m. Here, b is a 4-vector time series with component variables in $V_{\rm C}, I_{\rm pump}, I_{\rm S}, I_{\rm Na}$. It is generated either without the external forcing current, i.e. $I_{\rm ext} = 0$, or with a constant offset value as a parameter.

Signal: Only the net ion pump current $I_{\rm pump}(t)$ from the encoding time series b is chosen to be the signal through a transmission channel. In terms of neurophysiology, this amounts to assuming that only the active ion pump current is reproduced and propagated along the axon from the transmitting neuron to the receiving neuron. Denote the signal by $I_m(t) := I_{\rm pump}(t)$ with m corresponding to the message m.

Decoder: Let $\tilde{I}_m(t)$ denote the signal $I_m(t)$ after it goes through the transmission channel and appears at the input end of the receiver/decoder. Then the decoder is an $\tilde{I}_m(t)$-forced circuit, consisting of only the passive components of a $\text{pK}^+_-\text{sNa}^+_+$ circuit model:

$$\begin{cases} C{V_{\rm C}}' = -[I_{\rm Na} + f_{\rm K}(V_{\rm C} - \bar{E}_{\rm K}) + \sigma \tilde{I}_m(t) - I_0] \\ \epsilon {I_{\rm Na}}' = V_{\rm C} - \bar{E}_{\rm Na} - h_{\rm Na}(I_{\rm Na}). \end{cases} \tag{3}$$

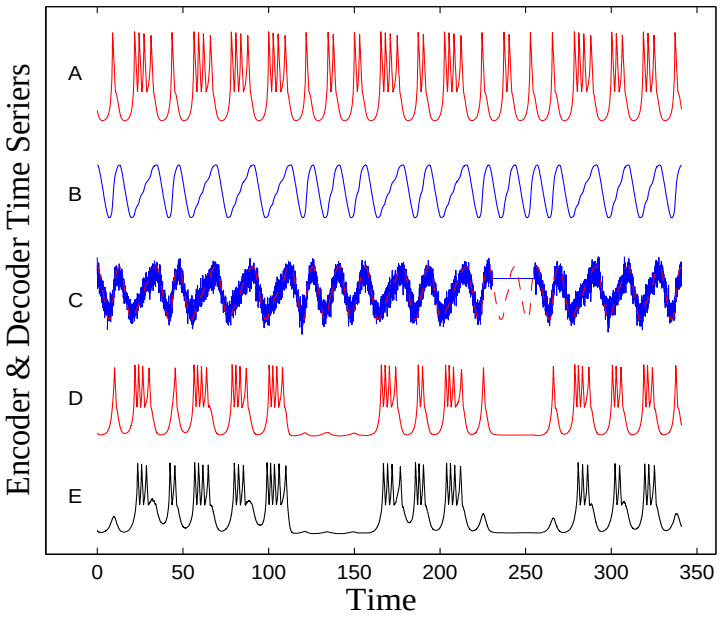

Figure 2: A typical simulation of SEED systems.

Here $\sigma\tilde{I}_m(t) - I_0$ can be thought as an external forcing current to the passive circuit, and parameters $\sigma,\ I_0$ as the decoder's tuning parameters. Other parameters can be used for tuning as well, examples include parameter $d_{\rm K}$ of the decoder circuit (3). The decoder circuit above does not have to share the same parameter values nor the same IV-characteristics $f_{\rm K}, h_{\rm Na}$ as the encoder circuit (1).

For the decoder to function as a such, and therefore for the SEED to work as a communication system, the pivotal question is can the decoder's forced membrane voltage $V_{\rm C}$ behave the same as the encoder's counterpart? Fig.2 shows the simulation of a SEED system. First a message is generated randomly in per-burst spike numbers: 14144412242412114331. The encoder's time-series representing the discrete message in the membrane potential $V_{\rm C}$ is shown by plot (A) and in the signal $I_m(t)$ by plot (B). Plot (C) shows $\tilde{I}_m(t)$, a modified version of the signal $I_m(t)$ by a noisy channel, including a random and complete signal loss between the 230 and 260 time marks for the 14th and the 15th signal symbols. Plot (D) shows the decoder's time-series in variable $V_{\rm C}$ from the noisy and degraded signal $\tilde{I}_m(t)$ of (C). In this simulation, the decoder is turned off intentionally but randomly between the 115 and 165 time marks. We can see that the original message is recovered by the spike-burst train (D) except those lost to transmission and system downtime. Plot (E) shows an errant decoding of the message when the decoder is mistuned to one set of the tuning parameters σ, I_0. We note that the decoder circuit is purposely made different from the passive components of the encoder circuit.

The conclusion is that a simple, reliable, and robust communication system can indeed be constructed from circuit models of single neurons, *using the transmitter neuron's active ion pump current as the system's signal waveform*.

Table 2: Definitions for Communication System Parameters

$\mathcal{A}_n = \{b_1, b_2, \ldots, b_n\}$	—	System alphabet for encoding, transmitting, and decoding.
$\tau = \{\tau_1, \tau_2, \ldots, \tau_n\}$	—	Base transmitting/processing time τ_k for base b_k.
$p = \{p_1, p_2, \ldots, p_n\}$	—	Probability distribution over $\mathcal{A}_n$ for an encoded source.
$H(p) = \sum_{k=1}^{n} p_k \log_2 \dfrac{1}{p_k}$	—	Averaged information entropy in bit per symbol of a particular source with encoded distribution p.
$T(p,\tau) = \sum_{k=1}^{n} p_k \tau_k$	—	Averaged transmitting/processing time per symbol of a particular source with encoded distribution p.
$R(p,\tau) = H(p)/T(p,\tau)$	—	Particular transmission rate in bit per time of a particular source with encoded distribution p.
$H_n = \log_2 n$	—	Maximal entropy $H_n = \max_p\{H(p)\}$ with the equiprobability distribution, $p_k = 1/n,\ 1 \le k \le n$, for all possible sources.
$R_n(\tau) = H_n / \sum_{k=1}^{n} \tau_k/n$	—	Mean transmission rate in bit per time for all sources with the equiprobability distribution.
$K_n(\tau) = \max_p\{R(p,\tau)\}$	—	Channel capacity with $p_k = p_1^{\tau_k/\tau_1},\ \sum_{k=1}^{n} p_1^{\tau_k/\tau_1} = 1$.

4. Optimal Quadrary Code. From a practical point of view, a communication system is only able to use a finite system alphabet $\mathcal{A}_n$ (see Table 2) to encode a given source whose messages are sequences of its source alphabet $\mathcal{S}_\ell = \{s_1, s_2, \ldots, s_\ell\}$. A source-to-channel encoding is a mapping from the source alphabet $\mathcal{S}_\ell$ to the set of finite sequences of the system alphabet $\mathcal{A}_n$ so that a source sequence in $\mathcal{S}_\ell$ is translated to a sequence in $\mathcal{A}_n$ for processing. A particular source when source-to-channel coded in $\mathcal{A}_n$ is characterized by a probability distribution p over the system alphabet, with p_k being the 1st order approximation of the probability to find base b_k at any position of the encoded messages. According to the information theory, base b_k contains $\log_2(1/p_k)$ bit of information for the encoded source, and a typical base on average contains $H(p)$ bit of information for the encoded source. In statistical mechanics, the quantity entropy, $H(p)$, is a measure of the disorder of particle states, and in information theory, it is the first order measure of the diversity of the encoded source. It is a simple and basic fact that the maximal entropy is reached if and only if at the equiprobability distribution $p_k = 1/n,\ 1 \le k \le n$ when each base occurs equally probable, and the maximal entropy is $H_n = \log_2(n)$.

From the point view of a communication system, animal brains in particular, the system is not designed for a *particular* source with a particular encoded distribution p, but rather for *all* possible sources. For example, the Internet is not designed for a particular source but rather for all sources, such as emails, pictures, videos, talk-show radios, and spams, just to name a few. In other words, it is only reasonable to assume that each base b_k will be used by some source, and it will be used equally likely when averaged over all sources. Symmetrically, from the perspective

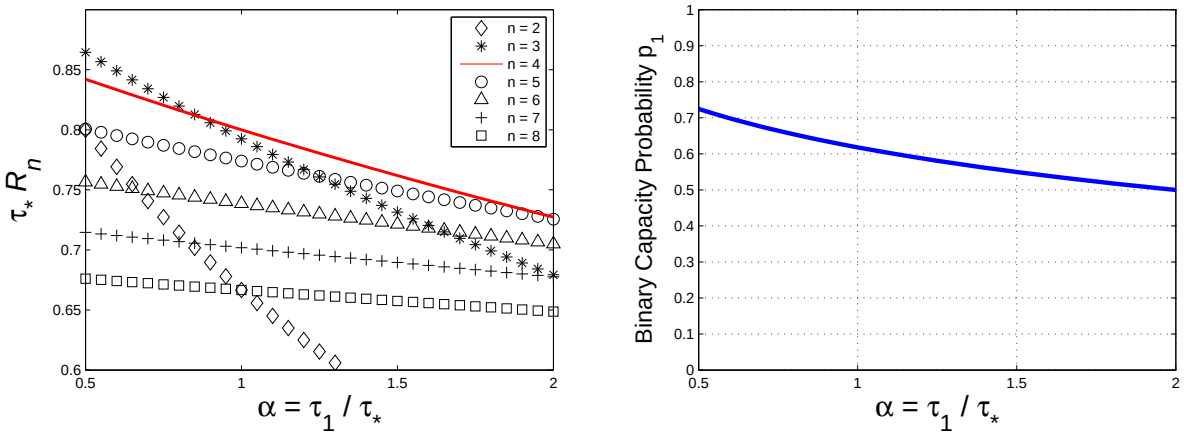

(a) (b)

Figure 3: (a) Mean Rate Comparison. R_4 seems to be the likely optimal solution for most practical choices of α. (b) Channel capacity probability p_1. For $\alpha = 1$, $p_1 = \Phi = 0.6180$ is the Golden Ratio.

of information sources, a communication system is just a black box whose internal parameters, such as the time cost to transmit the alphabetical bases, are in general unknown or oblivious to most sources, and therefore each alphabetical base of the system is as probable or as good to use as any others. In conclusion, for any n-alphabet communication system, the maximal information entropy $H_n = \log_2(n)$ in bit per base is a system-wise and source-determined payoff measure for the alphabet.

This does not mean that the larger the alphabet size the better the system. The balance lies in the consideration of the payoff against cost. The primary cost is the time the system takes to process the alphabet, such as to represent or to transmit a typical base. More specifically, a base b_k takes a fixed amount of time, τ_k, to process each time it occurs. For the equiprobability distribution, the average processing time is $T_n(\tau) = \sum_{k=1}^{n} \tau_k/n$ in time per base. Hence, the key performance parameter for a n-alphabet communication system is this payoff-to-cost ratio $R_n(\tau) = H_n/T_n(\tau)$ in bit per time, referred to as the *mean transmission rate* or the *transmission rate* for short. This is an intrinsic measure for all communication systems, regardless of the size nor the nature of their alphabets. As a result, different systems can be objectively compared. In the example of Internet, the transmission rate is the measure we use to compare different means of connection, such as DSL, coaxial cable, or satellite connections. Notice also that the mean transmission rate is partly determined by all possible *external* sources, and it is in this sense that the transmission rate is a *passive* measurement of a communication system.

Therefore, among the class of SEED systems, the decision criterion for the best system is to determine the alphabet size n so that the mean transmission rate R_n is maximal. To this end, we only need to use the spike-burst time relation (2) to calculate the average per-base transmitting

time T_n. Since $\tau_k = k\tau_*, \tau_1 = \alpha\tau_*$ for $k \geq 2$, we have by the formula $\sum_{k=1}^{n} k = (n+1)n/2$,

$$R_n(\tau) = \frac{H_n}{T_n(\tau)} = \frac{\log_2 n}{\tau_*[\frac{\alpha-1}{n} + \frac{n+1}{2}]}.$$

Fig.3(a) is a plot for the dimensionless or the time-normalized rate $\tau_* R_n$ as a function of $\alpha \in [0.5, 0.85]$ for $2 \leq n \leq 8$. It shows that the α range of $[0.5, 0.85]$ gives the best transmission rate by the ternary SEED system and $[0.85, 2]$ is the optimal range by the quadrary SEED system. Thus, for the circuit of Fig.1(c) with $\alpha = 0.95$, R_4 gives the best mean rate whereas for the circuit of Fig.1(d) with $\alpha = 0.80$, R_3 does instead.

5. Channel Capacity in Golden Ratio Distribution. From the perspective of a particular source, its particular payoff-to-cost ratio is the *source transmission rate* $R(p, \tau) = H(p)/T(p, \tau)$ with p being its encoded distribution over the system alphabet $\mathcal{A}_n$. Depending on the particular distribution p, this rate may be greater or smaller than the system mean rate $R_n(\tau)$. In other words, there is a potential gain for a particular source or a particular source-to-channel encoding scheme to exploit so that its particular rate $R(p, \tau)$ is no worse than all other sources. The mathematical problem is to maximize the source transmission rate $R(p, \tau)$ over all choices of the distribution p. The following is a variation of Shannon's result from [12].

Theorem 1. *For a n-alphabet communication system, its source transmission rate $R(p, \tau) = H(p)/T(p, \tau)$ can reach a unique maximum $K_n(\tau) = \max_p\{R(p, \tau)\}$ with respect to the encoded source distribution p. Specifically, the maximal solution p is the solution to the following equations,*

$$p_k = p_1^{\tau_k/\tau_1} \text{ for } 1 \leq k \leq n \text{ and } \sum_{k=1}^{n} p_1^{\tau_k/\tau_1} = 1, \tag{4}$$

and the maximal rate, referred to as the channel capacity, is $K_n(\tau) = -\log_2 p_1/\tau_1$.

Proof. Since the maximization is independent from the base presenting time τ, we will drop all references of it from the function T and R. The proof is based on the Lagrange multiplier method to maximize $R(p)$ subject to the constraint $g(p) = \sum_{k=1}^{n} p_k = 1$. This is to solve the joint equations: $\nabla R(p) = \lambda \nabla g(p), g(p) = 1$, where ∇ is the gradient operator with respect to p and λ is the Lagrange multiplier. Denote $R_{p_k} = \partial R/\partial p_k$. Then the first system of equations becomes $R_{p_k} = [H_{p_k} T - H\tau_{p_k}]/T^2 = \lambda g_{p_k} = \lambda$, componentwise. Write out the partial derivatives of H and T and simplify, we have $-(\log_2 p_k + 1/\ln 2)T - H\tau_k = \lambda T^2$ for $k = 1, 2, \ldots, n$. Subtract the equation for $k = 1$ from each of the remaining $n-1$ equations to eliminate the multiplier λ and to get a set of $n-1$ new equations: $-(\log_2 p_k - \log_2 p_1)T - H(\tau_k - \tau_1) = 0$ which solves to $\log_2 \frac{p_k}{p_1} = R(\tau_1 - \tau_k)$ and hence $p_k = \eta^{\tau_1 - \tau_k} p_1$ for all k where $\eta = 2^R = 2^{H/T}$ or $H = T \log_2 \eta$. Next we express the entropy H in terms of η and p_1, τ_1:

$$\begin{aligned} H &= -\sum_{k=1}^{n} p_k \log_2 p_k = -\sum_{k=1}^{n} p_k[(\tau_1 - \tau_k)\log_2 \eta + \log_2 p_1] \\ &= -[\tau_1 \log_2 \eta - \sum_{k=1}^{n} p_k \tau_k \log_2 \eta + \log_2 p_1] = -[\tau_1 \log_2 \eta + \log_2 p_1] + T \log_2 \eta, \end{aligned}$$

where we have used $\sum_{k=1}^{n} p_k = 1$ and $T = \sum_{k=1}^{n} p_k \tau_k$. Since we have by definition $H = T \log_2 \eta$, cancelling H from both sides of the equation above gives $\log_2 p_1 + \tau_1 \log_2 \eta = 0$ and consequently $2^R = \eta = p_1^{-1/\tau_1}$ and $p_k = \eta^{\tau_1 - \tau_k} p_1 = p_1^{\tau_k/\tau_1}$. Last solve the equation $f(p_1) = g(p) = \sum_{k=1}^{n} p_1^{\tau_k/\tau_1} = 1$ for p_1. Since $f(p_1)$ is strictly increasing in p_1 and $f(0) = 0 < 1$ and $f(1) = n > 1$, there is a unique solution $p_1 \in (0, 1)$ so that $f(p_1) = 1$. The channel capacity $K_n = R(p) = -\log_2 p_1/\tau_1 = -\log_2 p_k/\tau_k$ follows. This completes the proof. □

We now consider a special case for binary information sources. A source-to-channel encoding from a binary alphabet $\mathcal{S}_2 = \{s_1, s_2\}$ to a SEED system is a mapping from $\mathcal{S}_2$ to the set of all finite concatenations of the SEED's spike-burst alphabet $\mathcal{A}_n$. For example, $s_1 \to b_1 b_2, s_2 \to b_3$ can be a source-to-channel encoding for which a 1-spike burst followed by a 2-spike burst represents the source symbol s_1 and a 3-spike burst represents the source symbol s_2. We will consider instead a trivial and the most efficient source-to-channel encoding scheme that $s_1 \to b_1$ and $s_2 \to b_2$. Then, the source distribution over the source binary alphabet is exactly the encoded distribution $\{p_1, p_2\}$ over the quadrary SEED alphabet. For this binary SEED subsystem, the channel capacity is given by the formula $K_2 = -\log_2 p_1/\tau_1$ with p_1 satisfying $p_1 + p_1^{\tau_2/\tau_1} = 1$. Since $\tau_2 = \frac{2}{\alpha}\tau_1$, the equation becomes $p_1 + p_1^{2/\alpha} = 1$. For the special case when the base transmitting time τ_1 is the same as the minimal per-spike transmitting time $\tau_* = \tau_2/2$ with $\alpha = 1$, the equation becomes $p_1 + p_1^2 = 1$, whose solution is the Golden Ratio $p_1 = \Phi = \frac{\sqrt{5}-1}{2} = 0.6180,\ p_2 = p_1^2$ and $p_1 + p_2 = 1$. Fig.3(b) shows the optimal solution p_1 to the capacity distribution equation $p_1 + p_1^{2/\alpha} = 1$ as a function of the parameter α. It shows that the channel capacity distribution p_1 stays near the Golden Ratio over a modest α range near $\alpha = 1$.

6. Effect of Refractory Period. In the simulation and analysis above, we have deliberately left out the refractory periods for all spike-bursts. We now show that their inclusion will not qualitatively change any result obtained above for the SEED systems.

To see this, we turn our attention again to Fig.1. Let r_k denote the refractory period for the k-spike burst with the minimal burst period τ_k which we have used throughout the discussion. The plot Fig.1(b) shows that the refractory:burst period ratio r_k/τ_k can be assumed to be a constant, $\xi > 0$, for all $k \geq 1$. That is, $r_k = \xi\tau_k$. Hence, the total time duration for the k-spike burst is this sum $d_k := \tau_k + r_k = (1 + \xi)\tau_k = (1 + \xi)k\tau_*$. For the same spike-burst choices, the relationship (2) holds for the total bursting time d_k:

$$d_1 = \alpha(1 + \xi)\tau_* \quad \text{and} \quad d_k = \frac{k}{\alpha} d_1 = k(1 + \xi)\tau_* \quad \text{for} \quad k \geq 2.$$

As a result, the transmission rate for the refractory-inclusive SEED system is only a scaled multiple of the rate for the burst-only SEED system as follows

$$R_n(d) = \frac{H_n}{T_n(d)} = \frac{\log_2 n}{\tau_*(1 + \xi)[\frac{\alpha-1}{n} + \frac{n+1}{2}]} = \frac{1}{1 + \xi} R_n(\tau),$$

and their dimensionless normalized rates are exactly the same, $\tau_*(1 + \xi)R_n(d) = \tau_* R_n(\tau)$. Therefore, the optimal ternary and quadrary solutions for the new systems remains unchanged. Similarly,

the channel capacity distribution p from equation (4) for the new systems remains unchanged as well since the ratios for the new base transmitting times are the same as the old: $d_k/d_1 = \tau_k/\tau_1$. The only quantitative difference for the new channel capacity is again a scale-down of the old as $K_n(d) = K_n(\tau)/(1+\xi)$. As for simulations of the new SEED systems, they look just like Fig.2 except that there is a varying refractory period between every pair of adjacent spike-bursts. However, for circuit models similar to Fig.1(d) for which the refractory:burst ratio for the 1-spike burst is lower than the rest, the optimal mean rate solution further leans towards the ternary system since the total minimal 1-spike burst duration d_1 becomes smaller still.

7. Frequency Modulation and The Energy Requirement of Spike Bursts. On the surface, the alphabetical information in the number of spikes of a bursting base appears to be transmitted by the SEED system. However, since the alphabetical spike-bursts are uniquely coded by the plastic values $I_{\mathrm{S},\,k}$ of the absolute ion pump current I_{S}, it must be the plastic information in I_{S} that is actually transmitted. Here is how this is done by the SEED system. Rewrite the individual ion pump current equations of Eq.(1) with $\delta = 1$ in terms of the net and the absolute ion pump currents to get the following equivalent equations,

$$\begin{cases} {I_{\mathrm{pump}}}' = \lambda I_{\mathrm{S}}[V_{\mathrm{C}} - \gamma I_{\mathrm{pump}}] \\ {I_{\mathrm{S}}}' = \lambda I_{\mathrm{pump}}[V_{\mathrm{C}} - \gamma I_{\mathrm{pump}}]. \end{cases}$$

The first equation clearly shows that the plasticity of I_{S} is *frequency-modulated* onto the signal variable I_{pump}. For example, the smaller the total ion pump current I_{S} is, the lower the frequency of the signal I_{pump} becomes. This can also be clearly seen from the signal plot (B) of the SEED simulation Fig.2 as well as from Fig.1. The frequency component of I_{pump} in $I_{\mathrm{S},\,k}$ (at the start of the k-spike burst base) can be derived from Fig.1(b,d). The plots show that, to a good degree of approximation, the reciprocal $1/I_{\mathrm{S},\,k}$ is scaled linearly against the spike number k for $k \geq 2$: $1/I_{\mathrm{S},\,k} - 1/I_{\mathrm{S},2} = \mu(k-2)$, for some constant μ. Rewrite it to have

$$I_{\mathrm{S},\,k} = \frac{I_{\mathrm{S},2}}{1 + \mu I_{\mathrm{S},2}(k-2)}. \tag{5}$$

This shows that the higher the spike number k is, the smaller the frequency-modulation in the plastic variable $I_{\mathrm{S},\,k}$ becomes.

By definition, the electrical power through a device is $P(t) = I(t) \cdot V(t)$ in watt or joule per unit time where I is the absolute current through the device and V is the voltage across the device, and the total energy consumed in a period of τ is $\int_0^\tau I(t) \cdot V(t)dt$ in joule. For a k-spike burst with initial $I_{\mathrm{S}}(0) = I_{\mathrm{S},0}$ and burst period $\tau = \tau(I_{\mathrm{S},0})$, the total energy is

$$\Delta E(I_{\mathrm{S},0}) := \int_0^{\tau(I_{\mathrm{S},0})} I_{\mathrm{S}}(t) \cdot V_{\mathrm{C}}(t)dt.$$

The burst energy plots in Fig.1 place each initial $I_{\mathrm{S}}(0)$ against its corresponding spike-burst energy. First, the plots show that most sharp drops from the maximum to the minimum in energy occur

during transitions from $(k+1)$-spike bursts to k-spike bursts. Second, the plots show that for $k \geq 2$, each k-spike burst of the minimal bursting period spends approximately the same amount of energy, implying that a spike of a larger spike-number burst is less energetic than a spike of a smaller spike-number burst. The trade-off of using more energy for fewer spikes in bursting bases is for a faster transmission rate of the SEED system.

8. Discussions. The SEED communication model is about an implementation of some optimal principles gleaned from circuit models of single neurons. It is also artificial in a sense different from commented about in the Introduction because it requires the intervention of an engineer to preset the base defining plasticity $I_{\rm S}$ at the special values $I_{{\rm S},k}$ for the minimal base transmitting times, which results in the preferred number of bases to be either 3 or 4 depending on the encoder circuit. The question is which number code is biologically more probable, assuming the SEED principle as a working hypothesis for the real neurons?

To this end, we can envision the following evolutionary scenario, assuming our circuit models good approximations of real neurons. Neurons evolve to have their k-spike bursts as short as possible so that condition (2) is approximated closer and closer. However, because of the stochastic nature inherent to all biological processes, it is unrealistic to expect the encoding plasticity $I_{\rm S}$ to be set to the special set $I_{{\rm S},k}$ every time or most of the time. Instead, the plasticity variable should be expected to take on any value in a practical range of the system that is divided into the 1-spike burst subrange, the 2-spike burst subrange,..., etc. as shown in Fig.1. That is, it is more natural to assume that a typical k-spike-bursting base takes an average $\bar{\tau}_k$ unit of time to process, with $k/\bar{\tau}_k$ being the average spike frequency as shown in Fig.1. From the average spike frequency plots, it seems reasonable to assume that the condition (2) approximately holds for the average burst time $\bar{\tau}_k$ and that the corresponding α values are even closer to 1 than the case with the minimal bursting time τ_k is. This implies that if the circuits are good models for real neurons, the likely preferred number of spike-burst bases is 4, and the likely preferred distribution for binary information sources is near the Golden Ratio distribution.

One critical ingredient that makes the SEED model to work like a communication system is its utilization of the active ion pump current $I_{\rm pump}(t)$ as the signal between its transmitter and receiver circuits. This suggests that for real neuron-to-neuron communication, it might be the active ion pump currents that is transmitted through the pre-synaptic axons rather than the spike train or spike-burst train we normally observe in the membrane potential variable $V_{\rm C}$, which for the SEED system is simply a aggregated response to pre-synaptic all ion pump signals.

The SEED model also implies the energy source that is required to propagate the neuronal signal through the axon: the intercellular ATPass that fuels all ion pumps. In general circuitry, high frequency bursts are often associated with high informational entropy and fidelity, while low frequency tonic oscillations are often associated with the opposites. The suggested link between the cellular ATPass and the neuronal communication implies that the informational gain in high entropy-to-time rate is matched by high per-spike cellular energy expenditure.

However reasonable these predictions may sound, it is difficult to verify them at this point since

we do not know how to separate the active ion pump currents from their passive counterparts in vitro. Nevertheless, the hypothesis of aggregated axonal ion pump current as the singling messenger can be further tested by a refined SEED model which includes a network of pre-synaptic neural circuits and one post-synaptic circuit and uses some aggregation of pre-synaptic axonal pulses as the driving signal to the receiver. More future improvements are also desirable. For example, the absence of a linear array of axonal circuits to simulate SEED's transmitting channel is one, although not so critical, missing piece. Understanding the functioning role of synapses is another missing piece. On the other hand, however, the plasticity property of the neural circuits is not fully utilized by the SEED model. The current version is simply a demonstration in principles.

Neural information can take on many different forms, such as the discrete timing of electrical pulses, the number of spikes per burst, the frequency of spikes, or others ([10]). We have only focused here our construction and analysis on the metastable-plastic spike-bursts as SEED's system alphabets. The construction, the analysis, all can be immediately extended to metastable-plastic pulses ([6]) for which the processing time τ_k represents the pulse period of an instantaneous cycle frequency satisfying $\frac{1}{\tau_k} = \frac{\alpha}{k}\frac{1}{\tau_1}$. The SEED architecture can also be extended to incorporate other types of encoding schemes, with the timing encoding being another distinct possibility.

Obviously, nature has build a communication system out of neurons. How do the SEED optimization principles for neuron-to-neuron communication connect to the larger nervous network is certainly beyond the scope of this paper. On the other hand, the following phenomena found at the neuropsychological end of the subject are hard to miss for speculation, which may not be completely baseless, especially when considering the fact that all external stimuli enter our nervous system through individual neuroreceptors.

Human's visual system is most sensitive to three colors plus dark-gray, which is adapted for vision in the dark ([7]). Many species of birds and tropical fish have a visual system ranging from 3 to 5 colors. Our auditory system seems to have an innate preference to the 4/4 (or 3/4) beat in music, to which it is also natural for our body to dance. Most spoken languages have 4 or 5 basic vowel sounds to carry the conversations, figuratively speaking. Without exception, all Chinese idioms have exactly 4 characters, somehow it just seems to sound right. For animal echolocation, some species of bats make hight pitched calls centered around 4 frequencies at 30, 60, 90, 120 kHz ([11]). We do tabulation in group of 5s with 4 vertical bars plus a diagonal bar across. Chinese do the same but with a 5-stroke character meaning square. In India, children use a base 4 system to learn counting. In these three cases of tabulation, the distribution of the counting numerals is precisely the equiprobability. And in all other cases, it calls for the brains to embrace all possible variations from the respective sources. There are more examples of preferred short-term memory capacity around 4 as documented in [9, 2]. The underlining hypothesis is that animal brains have a neurological tendency to maximize information entropy against time cost like the optimal quadrary SEED system does.

To make it a more compelling case, we certainly have to find the type of empirical source-to-channel encodings to map such stimuli onto spike-bursts for processing in the central ner-

vous system. Here is a probable candidate case for such a scenario. For the calling frequencies cited above for echolocation, the frequency-modulation relation (5) can be neatly fitted with $I_{\mathrm{S},1} = 120w, \mu = 1/I_{\mathrm{S},1}$ to give rise to the correct scaling progression $I_{\mathrm{S},4} = 30w$, $I_{\mathrm{S},3} = 60w, I_{\mathrm{S},2} = 90w, I_{\mathrm{S},1} = 120w$, where w is some scaling constant. This may or may not be a curious coincidence, but the hypothesis is not lost that underneath the appearance of neuronal communication in firing spikes lies the ultimate response, transfer, and relay in energy — from the external energy carried by stimuli to the biochemical energy used by neurons to the output energy produced by effector cells such as the muscle cell.

Information sources with the Golden Ratio distribution are many. One example is the Golden Sequence, 101101011011010110101..., which is generated by starting with a symbol 1 and iterating the sequence according to 2 rules: replace every symbol 1 in the sequence by 10 and replace every symbol 0 in the sequence by 1. The distribution $\{p_0, p_1\}$ of the symbols $\{0, 1\}$ along the sequence has the Golden Ratio distribution: $p_0 + p_1 = 1, p_0/p_1 = p_1/1 = \Phi$. This gives a perfect illustration of Shannon's Fundamental Theory of Noiseless Channel: assigning symbol 1 to the 1-spike burst base and symbol 0 to the 2-spike burst base for the source-to-channel encoding gives rise to the binary SEED system's channel capacity. Penrose's aperiodic tiling is another example with Golden Ratio distribution. In its simplest form, its bases consist of a 54-degree rhombus and a 72-degree rhombus. The frequencies with which the rhombi appear in the plane follow the Golden Ratio distribution ([1]). Again, a trivial but most natural source-to-channel encoding gives rise to the fastest source transmission rate in the binary SEED system.

A rectangular frame is uniquely defined by its height-to-width (aspect) ratio. A frame of the Golden Ratio is 1:1.6180=1:$1/\Phi$. To translate it into a statistical distribution over a binary source, both height and width need to be proportionated against the height-width sum. Thus, the width:sum fraction is $p_1 = 1/\Phi/(1 + 1/\Phi) = 1/(\Phi + 1) = \Phi$, the Golden Ratio, which in turn corresponds to $\alpha = 1$ if $\{p_1, 1 - p_1\}$ is the binary channel capacity distribution. The aspect ratio of a typical widescreen monitor is 10:16, corresponding to a $p_1 = 16/26 = 0.6154$ binary distribution, and $\alpha \sim 0.99$ for a SEED binary channel capacity. The aspect ratio of a high definition TV is 9:16, corresponding to a $p_1 = 16/25 = 0.64$ binary distribution, or $\alpha \sim 0.90$. All fall inside the R_4-optimal mean rate range and near the Golden Ratio distribution for binary channel capacities as shown in Fig.3. The hypothesis that our brain has a psychological bias or preference to a particular source can gain a greater empirical support if we can demonstrate that our horizontal and vertical perception of a rectangular frame is encoded by a binary SEED system, which of course is not an easy task. In any case, SEED's channel capacity result does put forth the hypothesis that single neurons are hardwired to have informational preferences to the most entropy processed in unit time.

The SEED model suggests that biocommunication is far from being binary. It suggests that if a future communication network is build like the animal nervous system, it will most likely not be a binary system which we use for all digital communications today. And if it is build with neuron-like circuits, it will probably have to model after the quadrary SEED system for the best

transmission rate. As a farther extrapolation, human-like artificial intelligence probable will have to possess some general hardwired entropical biases towards information sources, and to possess certain particular combination of the general biases to give it a particular individual preference to interact with the external environment.

The payoff-to-cost analysis used in this paper for the SEED systems was also used in other areas of mathematical biology. It was used in [3] to analyze the replication rate for DNA replication which is thought as a communication system when nucleotide bases are paired to their complementary bases in sequence along the template strand of a DNA molecule. Under the assumption that the kth pair take k times as long to pair as the 1st pair does, it was shown in [3] that having 2 pairs of 2 complementary bases each gives the maximal system data rate, also called the mean replication rate there. In this case, the quadrary system consists of the A-T pair and the G-C pair nucleotides. The method was also used in [4] to analysis the recombination rate for sexual reproduction when the parental DNA are exchanged and mixed in the offspring chromosomes. In this case, the cost is in getting a set of parents from a species population, and the 2-sex reproductive scheme gives the best recombination-entropy-to-cost ratio at the molecular level's diversity. In addition, for the particular mating scheme of multiparous mammals, [4] also showed that having a father from 4 possible males for each member offspring of a female's litter gives the best multiparous-entropy-to-cost ratio at the organismic level's diversity. These cases seem to support the entropical optimization idea ([4]) that biological systems are driven by evolution to maximize diversity entropies against cost in time. In plain words, life is to produce more of different varieties in the shortest time possible.

References

[1] de Bruijn, N.G., *Algebraic theory of Penrose's non-periodic tilings of the plane,* Indagationes Mathematicae, **43**(1981), pp.38-66, Kon. Nederl. Akad. Wetensch. Proc. Ser. A, **84**(1981).

[2] Cowan, N., *The magical number 4 in short-term memory: A reconsideration of mental storage capacity,* Behavioral and Brain Sciences, **24**(2001), pp.87–185.

[3] Deng, B., *Why is the number of DNA bases 4?,* Bulletin of Math. Biol., **68**(2006), pp.727–733.

[4] Deng, B., *The origin of 2 sexes through optimization of recombination entropy against time and energy,* Bulletin of Math. Biol., **69**(2007), pp.2105–2114.

[5] Deng, B., *Conceptual and circuit models of neurons,* Journal of Integrative Neuroscience, **8**(2009), pp.255–297.

[6] Deng, B., *Metastability and plasticity in some conceptual models of neurons,* Journal of Integrative Neuroscience, **9**(2010), pp.31–47.

[7] Boynton, R. M., Human Color Vision, Holt, Rinehart and Winston, New York, (1979).

[8] Kandel, E.R., J.H. Schwartz, and T.M. Jessell, Principles of Neural Science, 3rd ed., Elsevier, 1991.

[9] Miller, G.A., *The magical number seven, plus or minus two: Some limits on our capacity for processing information,* Psychological Review 63, **2**(1956), pp.81-97.

[10] Perkel, D.H., T.H. Bullock, *Neural coding*, Neurosci. Res. Prog. Sum. **3**(1968), pp.405–527.

[11] Pollack, G.D. and J.H. Casseday, The neural basis of echolaction in bats, Srpinger-Verlage, Berlin, 1989.

[12] Shannon, C.E., *A methematical theory of communication,* Bell System Technical Journal, **27**(1948), pp.379–423, and pp.623–656.

[13] Zigmond, M.J., F.E. Bloom, S.C. Landis, J.L. Roberts, and L.R. Squire, Fundamental Neuroscience, Academic Press, 1999.

Supplements. The figure below shows the simulations for two more different circuit models whose complete equations can be found in [5, 6]. Fig.4(a,b) show that the absolute minimal uni-spike period for all k-spike bursts can be the same for all $k \geq 2$ as discussed in the main text. Fig.4(c,d) show typical plots for spike-burst frequencies. In such cases, the maximal spike frequency for each class of k-spike bursts increases in k, and approaches a limit. The circuit choice for SEED system has such parameter values so that the maximal uni-spike frequency sequence stays constant for all $k \geq 2$ as shown in (a,b) and Fig.1. Such optimal parameter values are fairly easy to find.

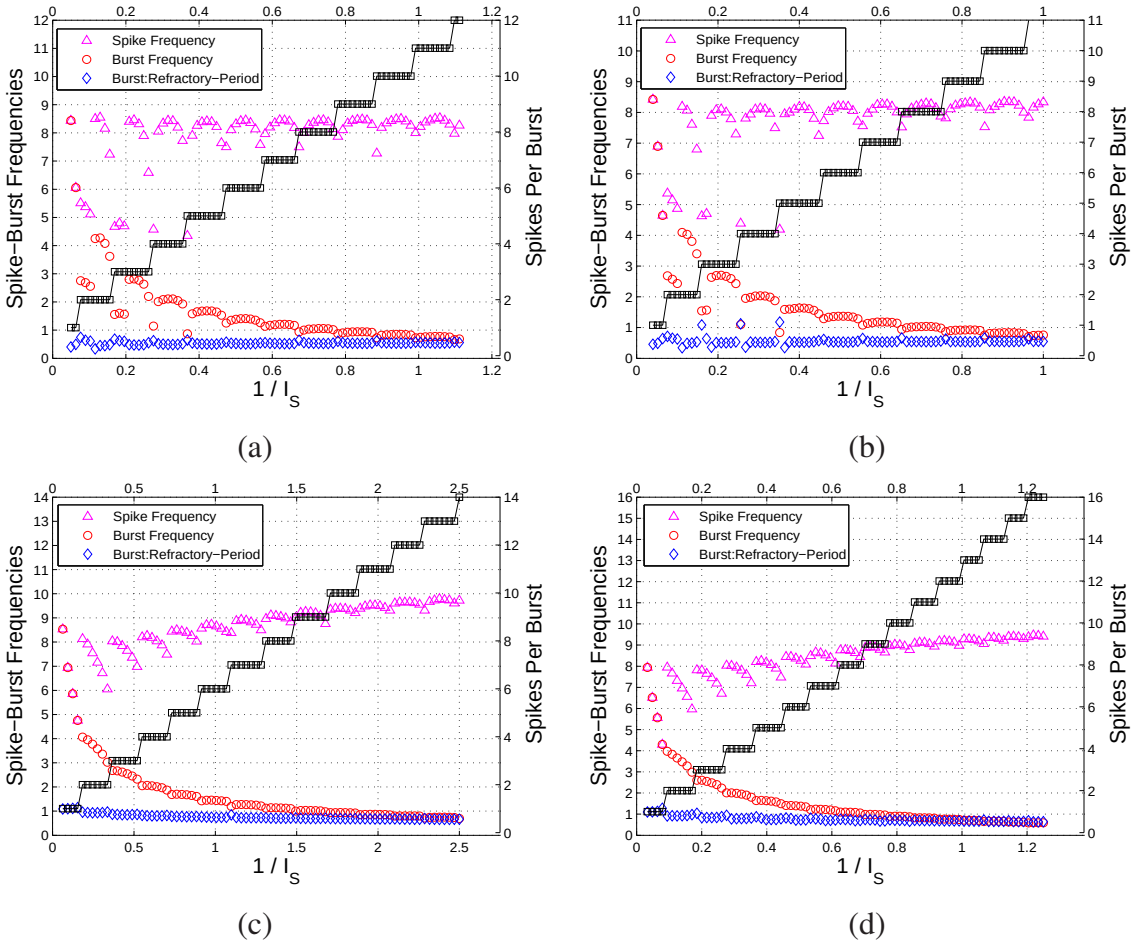

Figure 4: (a) $\text{pK}^+_-\text{sNa}^+_+$ model with the arctangent IV-curves. The same parameter values as Fig.1 except for $g_{\text{K}} = 5, d_{\text{K}} = -5.5, v_1 = 0.45, v_2 = 1.55, i_1 = .1, i_2 = 0.33, \lambda_{\text{Na}} = \lambda_{\text{K}} = 0.1$. (b) $\text{pK}^+_{-d}\text{sNa}^+_{+d}$ model with the arctangent IV-curves. The same parameter values as (a). (c) $\text{pK}^+_-\text{sNa}^+_+$ model with the cubic IV-curves. The same parameter values as Fig.1 except for $a = 1, v_1 = 0.5, v_2 = 2.5, b = 30, i_1 = 0.25, i_2 = 0.8, \lambda_{\text{Na}} = \lambda_{\text{K}} = 0.5$. (d) $\text{pK}^+_{-d}\text{sNa}^+_{+d}$ model with the cubic IV-curves. The same parameter values as (c) except for $\lambda_{\text{Na}} = 0.5, \lambda_{\text{K}} = 0.1, \gamma_{\text{Na}} = 0.1, \gamma_{\text{K}} = 0.5$.